

Vibration and stability of axially loaded cracked beams

Murat Kisa*

Department of Mechanical Engineering, Faculty of Engineering, Harran University, Sanliurfa, Turkey

(Received May 9, 2011, Revised September 11, 2012, Accepted October 9, 2012)

Abstract. Structural defects such as cracks are the source of local flexibilities and cause deficiencies in structural resistance. In the engineering constructions, structural elements sometimes are subjected to axial loading. Therefore, besides crack ratios and locations, influence of applied load on the stability and dynamical characteristics should also be explored. This study offers a numerical technique for the vibration and stability analysis of axially loaded cracked beams. The model merges finite element and component mode synthesis methods. Initially, stability analysis is completed and then dynamical characteristics of beams are found. Very good conformities between outcomes of the current study and those in literature, give the confidence that proposed method is reliable and effective.

Keywords: finite element analysis; damage; failure assessment; stability; axial load

1. Introduction

Dynamical characteristics (natural frequencies and mode shapes) of axially loaded cracked beams are of substantial importance in many structures. Working conditions, environment, mechanical vibrations, long-term service or applied cyclic loads may result in the initiation of structural defects such as cracks in the structures. Accordingly, the determination of the effects of these deficiencies on the vibration safety and stability of the structures is an important task of engineers. Cracks in a structural element modify its stiffness and damping properties. In view of that, the modal data of the structure contain information relating to the position and size of the deficiency. Vibration analysis allowing online inspection is an attractive method to detect cracks in the structures. As the interest in the non-destructive damage assessment of engineering structures from the vibration characteristics is continuously increasing, the effects of the cracks on the dynamical behaviour of the structures have been the subject of many researchers in the past (Gounaris and Dimarogonas 1988, Krawczuk and Ostachowicz 1993, Ruotolo *et al.* 1996, Kisa *et al.* 1998, Shifrin and Ruotolo 1999, Kisa and Brandon 2000, Morassi 2001, Viola *et al.* 2001, Krawczuk 2002, Patil and Maiti 2003, Kisa 2004, Zheng and Kessissoglou 2004, Kisa and Gurel 2007, Patel and Darpe 2009, Cheng *et al.* 2011, Pandey and Benipal 2011).

By means of the perturbation method as well as transfer matrix approach the effects of small cracks on the natural frequencies of slender structures were examined by Gudmundson (1983). Yuen (1985) proposed a methodical finite element process to set up the correlation between damage

*Corresponding author, Professor, E-mail: mkisa@harran.edu.tr

location, damage size and the corresponding alteration in the eigenparameters of a cantilever beam. Qian *et al.* (1990) developed a finite element model of an edge-cracked beam. Rizos *et al.* (1990) denoted the crack as a massless rotational spring, whose stiffness was computed by making use of the fracture mechanics. Dilena and Morassi (2001) investigated the analogous problem of a thin beam in bending vibration analytically and experimentally. They identified the crack location in vibrating beams from changes in node positions. Loya *et al.* (2006) determined the natural frequencies for bending vibrations of Timoshenko cracked beams with simple boundary conditions. They first established the differential equations for the free bending vibrations and then solved individually for each segment with the corresponding boundary conditions and appropriate compatibility conditions at the cracked section. Darpe (2007) presented a finite element model of a rotor with slant crack. In this model a new flexibility matrix for the slant crack is derived based on the fracture mechanics. Chasalevris and Papadopoulos (2008) studied the coupled bending vibrations of a stationary shaft with two cracks. In their study, they focus on the horizontal and vertical planes of a cracked shaft, whose bending vibrations are caused by a vertical excitation in the clamped end of the model.

The effects of axial load on the vibration characteristics of cracked beams have been studied by a few researchers. Takahashi (1998) analysed the vibration and stability of a non-uniform cracked shaft subjected to a tangential follower force by using the transfer matrix method. Zheng and Fan (2003) studied the vibration and stability of cracked hollow-sectional beams. Wang (2004) presented a comprehensive analysis of the stability of a cracked beam subjected to a follower compressive load and obtained buckling load of the cracked beam through dynamic analysis of the beam. Hsu (2005), by using the differential quadrature method (DQM), numerically formulated the eigenvalue problems of clamped-free and hinged-hinged Bernoulli-Euler cracked beams on elastic foundation with axial force. Binici (2005) investigated the vibration of beams with multiple open cracks subjected to axial force. His method uses one set of end conditions as initial parameters for determining the mode shape functions. Mei *et al.* (2006) presented wave vibration analysis of an axially loaded cracked beam considering the effects of shear deformation and rotary inertia. Arbodela-Monsalve *et al.* (2007) investigated the stability and free vibration analyses of a Timoshenko beam-column with generalised end conditions subjected to constant axial load and weakened by a cracked section along its span. They included the detrimental effects of a single weakened section and the beneficial effects of a lateral bracing located at the discontinuity. Viola *et al.* (2007) studied the free vibration of axially loaded cracked Timoshenko beam structures. They introduced a new procedure based on the coupling of dynamic stiffness matrix and line-spring element to model the cracked beam. Aristizabal-Ochoa (2007) proposed a model to analyse the static and dynamic stability of uniform shear beam-columns under generalised boundary conditions. This model includes the combined effects of shear deformations, an axially applied load linearly distributed along beam span, the translational and rotational inertias of the member's mass and of the rotational and translational lumped masses located at the ends of the member. Yang *et al.* (2008), by employing the modal series expansion technique, presented an analytical method to investigate the free and forced vibration of cracked inhomogeneous Euler-Bernoulli beams under an axial force and a moving load.

Aydin (2007, 2008) proposed a simple and efficient analytical approach to determine the vibratory characteristics of axially loaded Timoshenko and Euler-Bernoulli beams with arbitrary number of cracks. In the study, the local compliance induced by a crack was described by a massless rotational spring and a set of boundary conditions were used as initial parameters to define the mode shapes

of the segment of the beam before the first crack. Recently, Kukla (2009) investigated the free vibration and stability of stepped columns with cracks. The cracks in the column were modelled by massless rotational springs and the frequency equation was obtained by using the Green's functions.

Brandon and Abraham (1995) presented a method utilising substructure normal modes to predict the vibration properties of a beam with a closing crack. A method known as component mode synthesis or substructure technique, proposed by Hurty (1965), enabled the problem to be broken up into separate elements and thus considerably reduced its complexity. The advantage of the method in the case of a non-linear cracked beam stems from the fact that, when a beam is split into components from the crack sections, each substructure becomes linear and analytical or numerical results are available for their normal modes. Consequently, the initial non-linear system with local discontinuities in stiffness at the crack sections is now composed of a number of linear segments. An important characteristic of the model developed in this study is that it allows discontinuity in the displacement field at the crack section when the crack is open. Substructures are connected by artificial and massless springs whose stiffness coefficients are functions of the compliance coefficients. To the best of the author's knowledge, the presented method is applied for the first time to the cracked beams subjected to axial loading.

2. Theoretical development of the model

Consider an axially loaded cantilever beam, of uniform cross section, having an open transverse edge crack of depth r at a variable position L_c (Fig. 1). In the current study the crack faces assumed to be smooth and do not breathe during the vibration. The beam has a crack; therefore it is separated into two components from the crack section leading to a substructure methodology. Accordingly, as aforementioned, the global non-linear system with local stiffness discontinuities is detached into two linear subsystems. Each part is also broken up into finite elements with two nodes and three degrees of freedom at the every node as illustrated in Fig. 2.

2.1 Evaluation of local flexibility matrix of a cracked beam with rectangular cross section

A structural imperfection such as a crack in structures is a source of local flexibility which has effects on the dynamic properties of the structures. In the linear elastic range, these flexibility

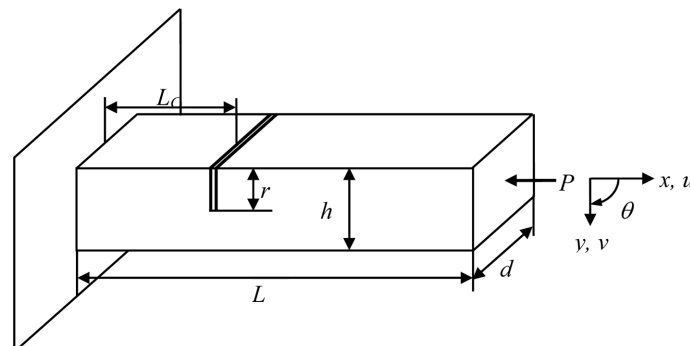


Fig. 1 Axially loaded cracked cantilever beam

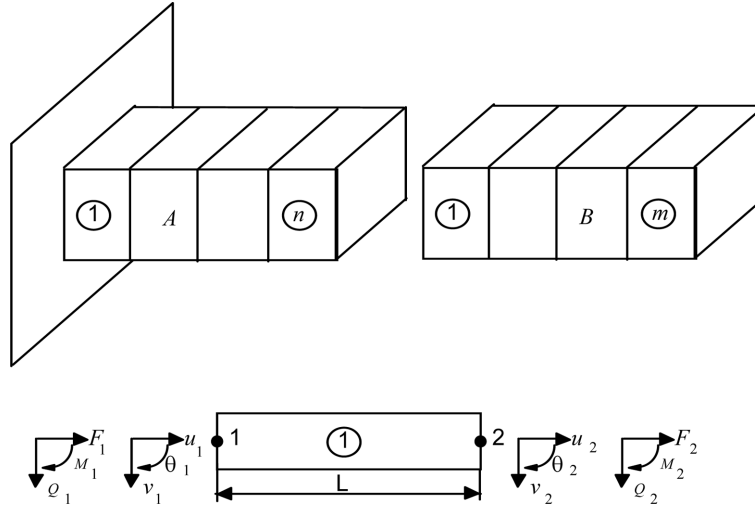


Fig. 2 Finite element model of the cracked beam

coefficients are expressed by stress intensity factors derived through Castigliano’s theorem. The strain energy release rate, J , represents the elastic energy in relation to a unit increase in length ahead of the crack front. For plane strain, J can be given as (Irwin 1960)

$$J = \frac{1-\nu^2}{E} K_I^2 + \frac{1-\nu^2}{E} K_{II}^2 + \frac{1+\nu^2}{E} K_{III}^2 \tag{1}$$

where K_I , K_{II} , K_{III} , ν and E are the stress intensity factors for the modes I , II , III deformation types, Poisson’s ratio and modulus of elasticity, respectively. In the current work, since the torsional effects are not considered, only mode I and mode II deformation types are taken into account. Let U be the strain energy of a cracked structure with a crack area A_C under the nodal loads P_i ($P_1 = F$, $P_2 = Q$, $P_3 = M$) then the relation between J and U is

$$J = \frac{\partial U(P_i, A_C)}{\partial A_C} \tag{2}$$

In accordance with the Castigliano’s theorem, the additional displacement caused by the crack in the direction of P_i can be given as

$$u_i = \frac{\partial U(P_i, A_C)}{\partial P_i} \tag{3}$$

Substituting Eq. (2) into Eq. (3) gives the final expression between displacement and strain energy release rate J as

$$u_i = \frac{\partial}{\partial P_{iA}} \int J(P_i, A_C) dA_C \tag{4}$$

Now the flexibility coefficients which are the functions of the crack shape and the stress intensity factors can be introduced as follows

$$c_{ij} = \frac{\partial u_i}{\partial P_j} = \frac{\partial^2}{\partial P_i \partial P_j} \int_A J(P_i, A_C) dA_C \quad (5)$$

The flexibility coefficients c_{ij} are obtained from the fracture mechanics method proposed by Dimarogonas and Paipetis (1983). Dimensionless flexibility coefficients are calculated numerically. Since the shear force does not contribute to the opening mode of the crack, the flexibility matrix, in relation to displacements (u, v, θ) , can be written as

$$\mathbf{C} = \begin{bmatrix} c_{11} & 0 & c_{13} \\ 0 & c_{22} & 0 \\ c_{31} & 0 & c_{33} \end{bmatrix}_{(3 \times 3)} \quad (6)$$

Using the flexibility matrix, the stiffness matrix induced by a crack is given as

$$\mathbf{K}_{cr} = \begin{bmatrix} \mathbf{C}^{-1} & -\mathbf{C}^{-1} \\ -\mathbf{C}^{-1} & \mathbf{C}^{-1} \end{bmatrix}_{(6 \times 6)} \quad (7)$$

2.2 Component mode analysis

Consider an axially loaded component A , whose equation of motion in matrix notation can be given as follows

$$\mathbf{M}_A \ddot{\mathbf{q}}_A + \mathbf{D}_A \dot{\mathbf{q}}_A + \mathbf{K}_A \mathbf{q}_A + P \mathbf{K}_{GA} \mathbf{q}_A = \mathbf{f}_A(t) \quad (8)$$

where \mathbf{M}_A , \mathbf{D}_A , \mathbf{K}_A , \mathbf{K}_{GA} , P , \mathbf{q} and $\mathbf{f}_A(t)$ are the mass matrix, damping matrix, stiffness matrix, geometric stiffness matrix, applied compressive load, generalised displacement vector and external force vector, respectively, for the component A . Well known geometric stiffness matrix can be given as follows

$$[\mathbf{K}_G] = \frac{1}{L} \begin{bmatrix} 0 & 0 & 0 & 0 & 0 & 0 \\ 0 & \frac{6}{5} & \frac{L}{10} & 0 & -\frac{6}{5} & \frac{L}{10} \\ 0 & \frac{L}{10} & \frac{2}{15}L^2 & 0 & -\frac{L}{10} & -\frac{L^2}{30} \\ 0 & 0 & 0 & 0 & 0 & 0 \\ 0 & -\frac{6}{5} & -\frac{L}{10} & 0 & \frac{6}{5} & -\frac{L}{10} \\ 0 & \frac{L}{10} & -\frac{L^2}{30} & 0 & -\frac{L}{10} & \frac{2}{15}L^2 \end{bmatrix} \quad (9)$$

For undamped free vibration analysis, Eq. (8) rewritten as

$$\mathbf{M}_A \ddot{\mathbf{q}}_A + (\mathbf{K}_A + P \mathbf{K}_{GA}) \mathbf{q}_A = 0 \quad (10)$$

Assuming that

$$\{\mathbf{q}\} = \{\boldsymbol{\varphi}\} \sin(\omega t + \beta), \quad \{\ddot{\mathbf{q}}\} = -\omega^2 \{\boldsymbol{\varphi}\} \sin(\omega t + \beta) \quad (11)$$

and substituting them into Eq. (10) gives the standard free vibration equation for the component A as

$$\omega^2 \mathbf{M}_A \boldsymbol{\varphi} = (\mathbf{K}_A + P\mathbf{K}_{GA}) \boldsymbol{\varphi} \quad (12)$$

which gives eigenvalues $\omega_{A1}^2, \dots, \omega_{An}^2$ and modal matrix $\boldsymbol{\varphi}_A$ for the component A . \mathbf{q}_A can be defined as principal coordinate vector \mathbf{p}_A by using the following relation

$$\mathbf{q}_A = \boldsymbol{\varphi}_A \mathbf{p}_A \quad (13)$$

Premultiplying Eq. (13) by $\boldsymbol{\varphi}_A^T$ and substituting it into Eq. (10) gives the following equation.

$$(\boldsymbol{\varphi}_A^T \mathbf{M}_A \boldsymbol{\varphi}_A) \ddot{\mathbf{p}}_A + (\boldsymbol{\varphi}_A^T (\mathbf{K}_A + P\mathbf{K}_{GA}) \boldsymbol{\varphi}_A) \mathbf{p}_A = 0 \quad (14)$$

where

$$\begin{aligned} \boldsymbol{\varphi}_A^T \mathbf{M}_A \boldsymbol{\varphi}_A &= [\mathbf{m}_m] \\ \boldsymbol{\varphi}_A^T (\mathbf{K}_A + P\mathbf{K}_{GA}) \boldsymbol{\varphi}_A &= [\mathbf{k}_m] \end{aligned} \quad (15)$$

where $[\mathbf{m}_m]$ and $[\mathbf{k}_m]$ are the modal mass and stiffness matrices, respectively. If the modal matrix is normalised by the mass, mass normalised mode vector $\boldsymbol{\psi}_{ij}$ can be given as

$$\boldsymbol{\psi}_{ij} = \frac{\boldsymbol{\varphi}_{ij}}{\sqrt{m_{jj}}} \quad (16)$$

\mathbf{q}_A can be defined as principal coordinate vector \mathbf{s}_A by using the following transformation

$$\mathbf{q}_A = \boldsymbol{\psi}_A \mathbf{s}_A \quad (17)$$

Premultiplying Eq. (17) by $\boldsymbol{\psi}_A^T$ and substituting it into Eq. (10) results in

$$(\boldsymbol{\psi}_A^T \mathbf{M}_A \boldsymbol{\psi}_A) \ddot{\mathbf{s}}_A + (\boldsymbol{\psi}_A^T (\mathbf{K}_A + P\mathbf{K}_{GA}) \boldsymbol{\psi}_A) \mathbf{s}_A = 0 \quad (18)$$

where

$$\begin{aligned} (\boldsymbol{\psi}_A^T \mathbf{M}_A \boldsymbol{\psi}_A) &= \mathbf{I} \\ (\boldsymbol{\psi}_A^T (\mathbf{K}_A + P\mathbf{K}_{GA}) \boldsymbol{\psi}_A) &= \boldsymbol{\omega}_A^2 \end{aligned} \quad (19)$$

Using Eq. (19), Eq. (18) becomes

$$\mathbf{I} \ddot{\mathbf{s}}_A + \boldsymbol{\omega}_A^2 \mathbf{s}_A = 0 \quad (20)$$

where $\boldsymbol{\omega}_A^2$ is a diagonal matrix comprising the eigenvalues of component A .

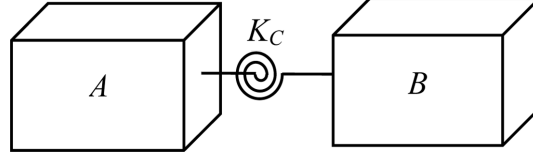


Fig. 3 Joining of two components by a spring

2.3 Joining procedure of the components

Consider two components A and B connected together via a spring, as illustrated in Fig. 3. Kinetic (T) and strain energy (U) of the two components, in terms of principal modal coordinates, can be given as

$$T = \frac{1}{2} \begin{Bmatrix} \dot{\mathbf{s}}_A \\ \dot{\mathbf{s}}_B \end{Bmatrix}^T \left(\begin{bmatrix} \boldsymbol{\Psi}_A & 0 \\ 0 & \boldsymbol{\Psi}_B \end{bmatrix}^T \begin{bmatrix} \mathbf{M}_A & 0 \\ 0 & \mathbf{M}_B \end{bmatrix} \begin{bmatrix} \boldsymbol{\Psi}_A & 0 \\ 0 & \boldsymbol{\Psi}_B \end{bmatrix} \right) \begin{Bmatrix} \dot{\mathbf{s}}_A \\ \dot{\mathbf{s}}_B \end{Bmatrix}$$

$$U = \frac{1}{2} \begin{Bmatrix} \mathbf{s}_A \\ \mathbf{s}_B \end{Bmatrix}^T \left(\begin{bmatrix} \boldsymbol{\Psi}_A & 0 \\ 0 & \boldsymbol{\Psi}_B \end{bmatrix}^T \begin{bmatrix} (\mathbf{K} + P\mathbf{K}_G)_A & 0 \\ 0 & (\mathbf{K} + P\mathbf{K}_G)_B \end{bmatrix} \begin{bmatrix} \boldsymbol{\Psi}_A & 0 \\ 0 & \boldsymbol{\Psi}_B \end{bmatrix} \right) \begin{Bmatrix} \mathbf{s}_A \\ \mathbf{s}_B \end{Bmatrix} \quad (21)$$

where

$$\begin{bmatrix} \boldsymbol{\Psi}_A & 0 \\ 0 & \boldsymbol{\Psi}_B \end{bmatrix}^T \begin{bmatrix} \mathbf{M}_A & 0 \\ 0 & \mathbf{M}_B \end{bmatrix} \begin{bmatrix} \boldsymbol{\Psi}_A & 0 \\ 0 & \boldsymbol{\Psi}_B \end{bmatrix} = \begin{bmatrix} \mathbf{I} & 0 \\ 0 & \mathbf{I} \end{bmatrix}$$

$$\begin{bmatrix} \boldsymbol{\Psi}_A & 0 \\ 0 & \boldsymbol{\Psi}_B \end{bmatrix}^T \begin{bmatrix} (\mathbf{K} + P\mathbf{K}_G)_A & 0 \\ 0 & (\mathbf{K} + P\mathbf{K}_G)_B \end{bmatrix} \begin{bmatrix} \boldsymbol{\Psi}_A & 0 \\ 0 & \boldsymbol{\Psi}_B \end{bmatrix} = \begin{bmatrix} \boldsymbol{\omega}_A^2 & 0 \\ 0 & \boldsymbol{\omega}_B^2 \end{bmatrix} \quad (22)$$

The strain energy of the connectors, in terms of principal modal coordinates, is

$$U_C = \frac{1}{2} \begin{Bmatrix} \mathbf{s}_A \\ \mathbf{s}_B \end{Bmatrix}^T \left(\begin{bmatrix} \boldsymbol{\Psi}_A & 0 \\ 0 & \boldsymbol{\Psi}_B \end{bmatrix}^T \mathbf{K}_C \begin{bmatrix} \boldsymbol{\Psi}_A & 0 \\ 0 & \boldsymbol{\Psi}_B \end{bmatrix} \right) \begin{Bmatrix} \mathbf{s}_A \\ \mathbf{s}_B \end{Bmatrix} \quad (23)$$

where \mathbf{K}_C is the connector matrix comprising the cracked nodal element's stiffness matrix which can be calculated by using Eq. (6). The total strain energy of the system is

$$U_T = \frac{1}{2} \begin{Bmatrix} \mathbf{s}_A \\ \mathbf{s}_B \end{Bmatrix}^T \left(\begin{bmatrix} \boldsymbol{\Psi}_A & 0 \\ 0 & \boldsymbol{\Psi}_B \end{bmatrix}^T \begin{bmatrix} (\mathbf{K} + P\mathbf{K}_G)_A & 0 \\ 0 & (\mathbf{K} + P\mathbf{K}_G)_B \end{bmatrix} \begin{bmatrix} \boldsymbol{\Psi}_A & 0 \\ 0 & \boldsymbol{\Psi}_B \end{bmatrix} + \begin{bmatrix} \boldsymbol{\Psi}_A & 0 \\ 0 & \boldsymbol{\Psi}_B \end{bmatrix}^T \mathbf{K}_C \begin{bmatrix} \boldsymbol{\Psi}_A & 0 \\ 0 & \boldsymbol{\Psi}_B \end{bmatrix} \right) \begin{Bmatrix} \mathbf{s}_A \\ \mathbf{s}_B \end{Bmatrix} \quad (24)$$

Using Lagrange's equation with Eqs. (21-24), the eigenvalue equation can be given as

$$\left(\begin{bmatrix} \boldsymbol{\omega}_A^2 & 0 \\ 0 & \boldsymbol{\omega}_B^2 \end{bmatrix} + \begin{bmatrix} \boldsymbol{\Psi}_A & 0 \\ 0 & \boldsymbol{\Psi}_B \end{bmatrix}^T [\mathbf{K}_C] \begin{bmatrix} \boldsymbol{\Psi}_A & 0 \\ 0 & \boldsymbol{\Psi}_B \end{bmatrix} - \boldsymbol{\omega}^2 \begin{bmatrix} \mathbf{I} & 0 \\ 0 & \mathbf{I} \end{bmatrix} \right) \begin{Bmatrix} \mathbf{s}_A \\ \mathbf{s}_B \end{Bmatrix} = \begin{Bmatrix} 0 \\ 0 \end{Bmatrix} \quad (25)$$

From Eq. (25) natural frequencies and mode shapes of the axially loaded cracked beam can be found. After solving this equation, the displacements for each component are calculated by using Eq. (17).

2.4 Buckling analysis

In the current study, for the free vibration analysis of the axially loaded cracked beams, a compressive axial load is applied to the cracked beam. The magnitude of the applied axial loading cannot exceed the critical buckling load and as a consequence before the free vibration analysis, a buckling analysis of the cracked beam is carried out for the determination of the critical buckling loads. In the buckling analysis, the magnitude of the axial load which causes buckling of the column is unknown. As previously given, the equation of motion for the free vibration of an axially loaded cracked beam, in matrix notation can be given as

$$\mathbf{M}\ddot{\mathbf{q}} + (\mathbf{K} + \mathbf{K}_C + P\mathbf{K}_G)\mathbf{q} = 0 \quad (26)$$

In the static case ($\ddot{\mathbf{q}} = 0$) Eq. (26) gives the typical buckling equation as

$$(\mathbf{K} + \mathbf{K}_C + P\mathbf{K}_G)\mathbf{q} = 0 \quad (27)$$

For a non-trivial solution, one can write

$$|(\mathbf{K} + \mathbf{K}_C) + \lambda\mathbf{K}_G| = 0 \quad (28)$$

This is an eigenvalue problem and the lowest value of λ will give the first critical buckling load (P_{cr}) for the cracked beam.

3. Numerically studied cases

3.1 Axially loaded fixed free cracked beam

As a first case, a fixed-free cracked beam subjected to compressive axial load (Fig. 4) is analysed. The geometrical possessions of the beam are taken as; length $L = 3$ m, height $h = 0.2$ m and width

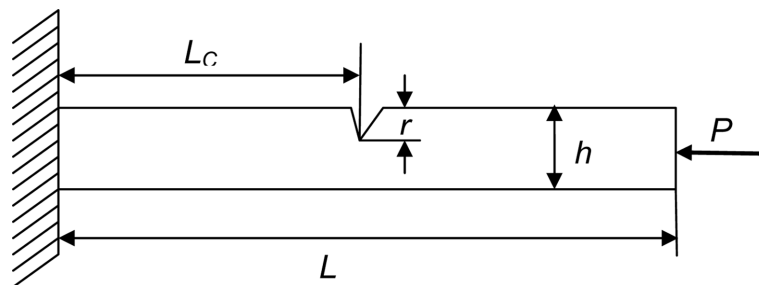


Fig. 4 A fixed-free axially loaded cracked beam

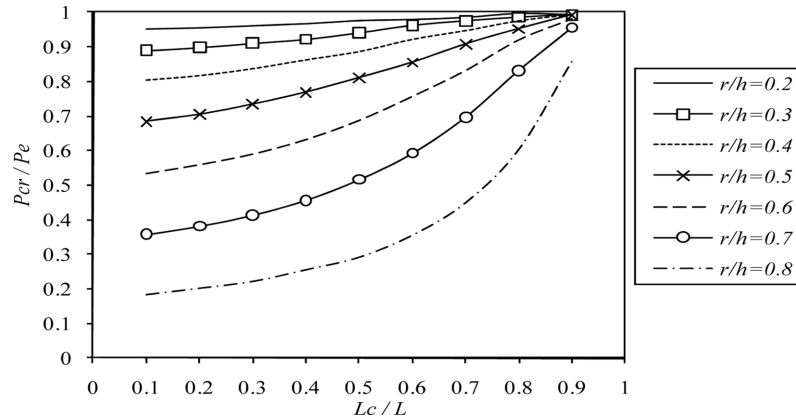


Fig. 5 First non-dimensional buckling load of cracked beam with respect to different crack locations (L_c/L) and crack ratios (r/h)

$d = 0.2$ m. Numerical calculation has been executed with the material properties; Young's modulus $E = 216 \times 10^9 \text{ N m}^{-2}$, Poisson's ratio $\nu = 0.33$ and material density $\rho = 7.85 \times 10^3 \text{ kgm}^{-3}$. Prior to vibration of axially loaded cracked beam, a buckling analysis is completed to find the critical buckling loads. Throughout this study only elastic buckling is considered.

3.1.1 Buckling analysis of fixed-free cracked beam

The fundamental critical buckling load of the fixed-free intact beam can be found by using the Euler formula as

$$P_e = \frac{\pi^2 EI}{4L^2} \tag{29}$$

Using Eq. (28) the principal critical buckling load of cracked beam is determined. The variations of the first non-dimensional buckling load (P_{cr}/P_e) of cracked beam with respect to different crack locations and ratios have been demonstrated in Fig. 5. P_{cr} and P_e stand for the principal buckling load of the cracked and intact beam, respectively. Cracks result in decreases in the critical buckling loads. Crack ratios and locations affect the buckling behaviour of the beam. As expected, larger cracks situated near the fixed end of the beam produces higher drops in the buckling load, for instance a relatively big crack ($r/h = 0.8$) near the fixed end ($L_c/L = 0.1$) reduces the fundamental buckling load about 80%. On the contrary, even it is comparatively big ($r/h = 0.6$), when a crack approaches to the free end it has little effects on the buckling load of the beam.

3.1.2 Vibration of axially loaded fixed-free cracked beam

As previously presented, crack and applied compressive axial load decrease the overall stiffness of the beam, as a consequence the dynamical characteristics of the beam are modified. Free vibration of axially loaded cracked beam is completed by using Eq. (25). To confirm the accuracy and reliability of the presented method the results of the current study and those of Binici's (2005) are compared and as can be seen from the Fig. 6, very good conformities have been found between them. In the analysis the crack ratio is taken to be $r/h = 0.5$. It is also apparent from the Fig. 6 that

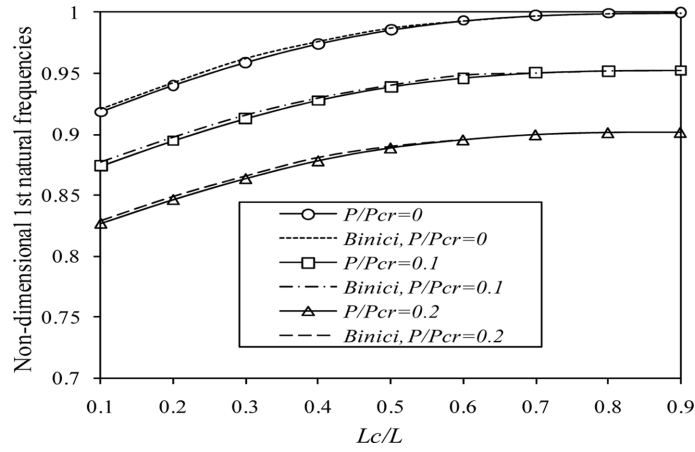


Fig. 6 Literature comparison of first non-dimensional natural frequencies of axially loaded fixed-free cracked beam

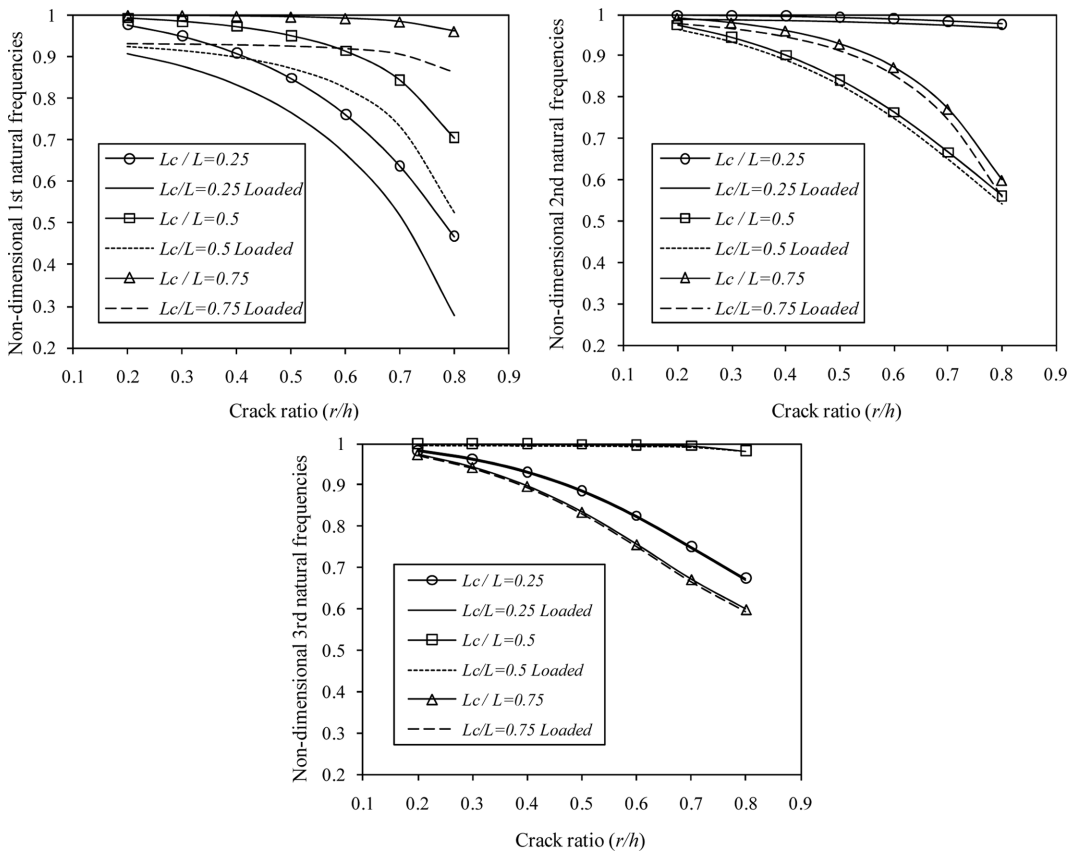


Fig. 7 First, second and third non-dimensional natural frequencies of cracked beam with respect to different crack locations (Lc/L) and crack ratios (r/h)

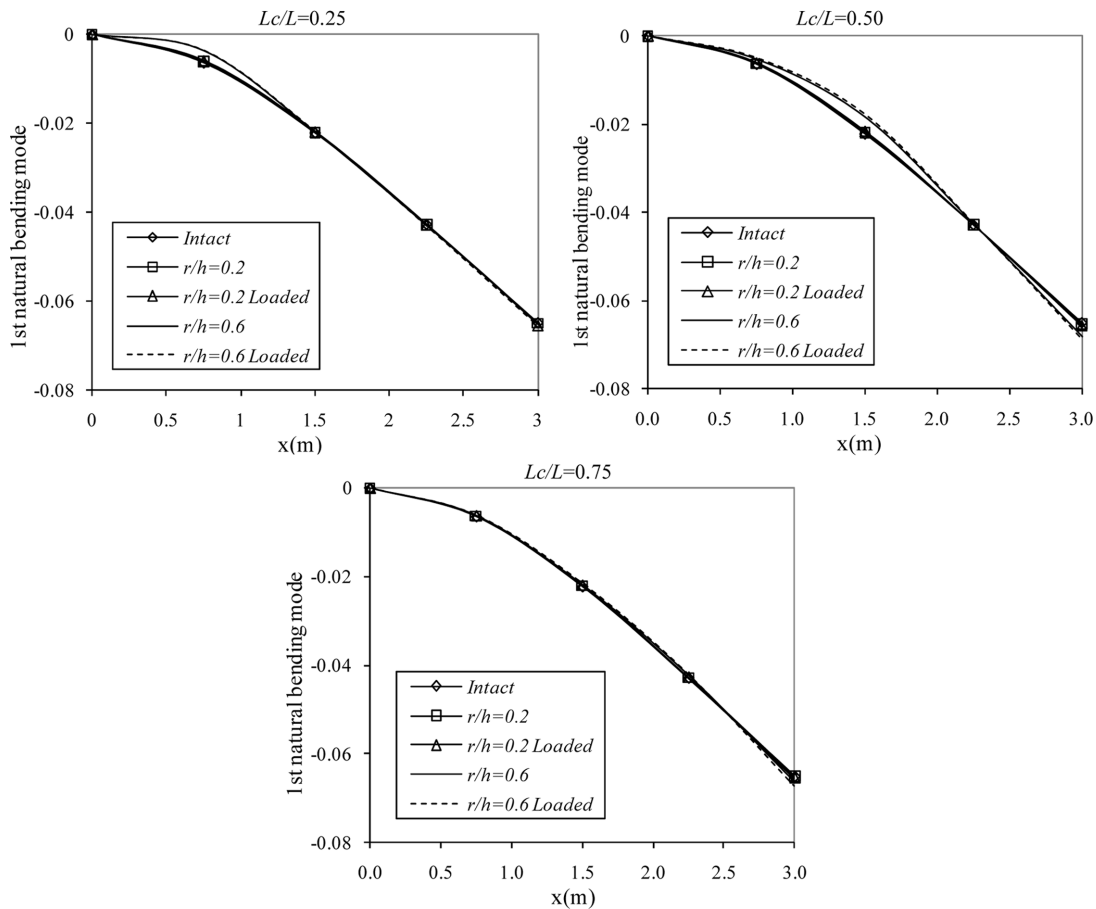


Fig. 8 First natural mode shapes of the fixed-free beam with respect to crack locations $Lc/L = 0.25, 0.50, 0.75$ and crack ratios $r/h = 0.2, 0.6$ for the intact, loaded and unloaded cracked beams

if the applied axial compressive load ratio gets higher, the frequency reductions also increase.

Confirming the reliability and correctness of the offered procedure gives the applicability of the method with a confidence. Now, the beam in Fig. 4 is considered and an axial load P ($P/P_{cr} = 0.1$) is applied and then the free vibration of the beam is carried out. The deviation of the first, second and third non-dimensional natural frequencies ($\omega_{cracked}/\omega_{intact}$) of axially loaded cracked beam with respect to different crack locations and ratios have been given in the Fig. 7.

It is observed from the figure that, crack locations, crack ratios and applied axial load levels strongly affect the natural frequencies of the beam. While a crack near the fixed end ($Lc/L = 0.25$) causes more effects on the first natural frequencies, a crack located at the middle ($Lc/L = 0.50$) and near the end of the beam ($Lc/L = 0.75$) result in more reductions in the second and third natural frequencies, respectively. Figure shows that an axial load ratio of 10% ($P/P_{cr} = 0.1$) can affect the first natural frequencies by about 8% compared to unloaded beam. This effect is observed to be fewer important for the second and third mode natural frequencies.

Variations of the first mode shapes of the fixed-free beam with respect to crack locations $Lc/L = 0.25, 0.50, 0.75$ and crack ratios $r/h = 0.2, 0.6$ for the intact, loaded and unloaded cracked beams

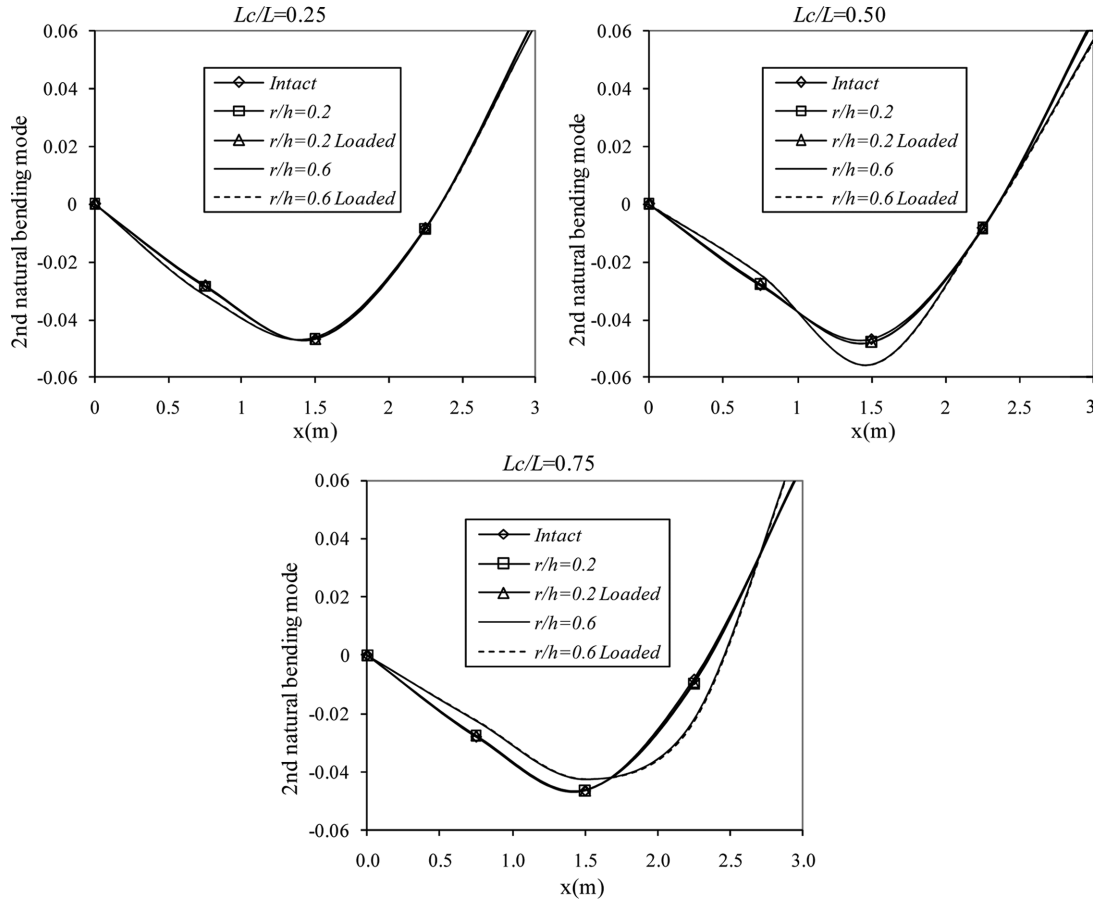


Fig. 9 Second mode shapes of the fixed-free beam with respect to crack locations $L_c/L = 0.25, 0.50, 0.75$ and crack ratios $r/h = 0.2, 0.6$ for the intact, loaded and unloaded cracked beams

are illustrated in Fig. 8. It is clear that a crack makes changes in the mode shapes, moreover an applied axial load results in additional alterations in the mode shapes. The crack locations also influence the mode shape changes. The position of the crack can be recognised from the mode shapes when the crack ratio gets higher.

Differences in the second mode shapes of the fixed-free beam with respect to crack locations $L_c/L = 0.25, 0.50, 0.75$ and crack ratios $r/h = 0.2, 0.6$ for the intact, loaded and unloaded cracked beams are demonstrated in Fig. 9. The effects of the crack locations, ratios and applied load are evident from the Fig. 9. While the big crack ($r/h = 0.6$) at the end of the beam ($L_c/L = 0.75$) has little effects on the first mode shapes and can not be recognised, it is noticeable from the figure that same crack has bigger effect on the second mode shapes and can be detected.

Variations of the third mode shapes of the fixed-free beam with respect to crack locations $L_c/L = 0.25, 0.50, 0.75$ and crack ratios $r/h = 0.2, 0.6$ for the intact, loaded and unloaded cracked beams are displayed in Fig. 10. A crack located at the middle of the beam ($L_c/L = 0.5$) has no influence on the third mode shapes as it has more effect on the second mode shapes. As a consequence, all mode shapes should be checked for crack detection process.

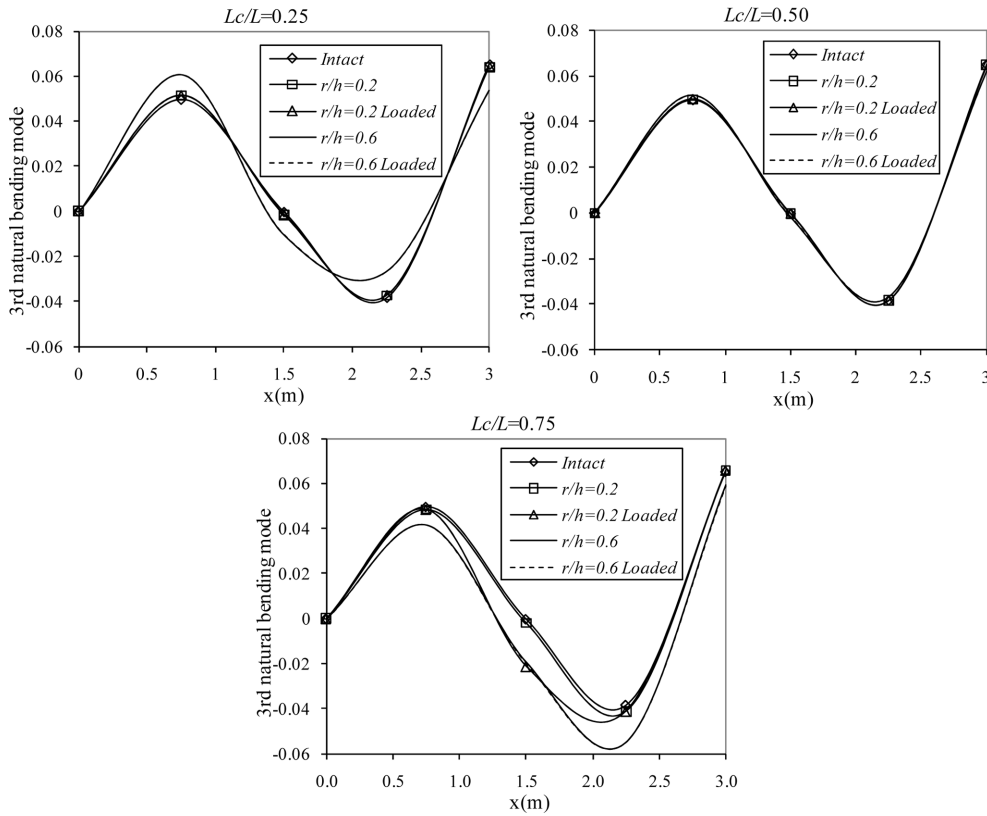


Fig. 10 Third mode shapes of the fixed-free beam with respect to crack locations $L_c/L = 0.25, 0.50, 0.75$ and crack ratios $r/h = 0.2, 0.6$ for the intact, loaded and unloaded cracked beams

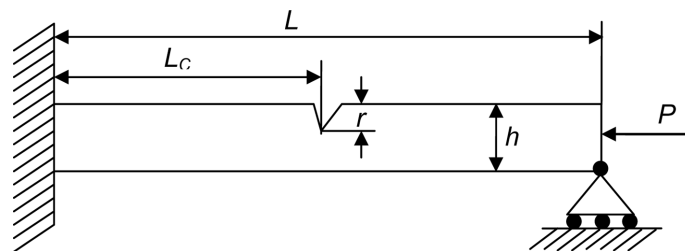


Fig. 11 A fixed-pinned axially loaded cracked beam

3.2 Axially loaded fixed-pinned cracked beam

Second sample is chosen as a fixed-pinned cracked beam subjected to axial loading (Fig. 11). The geometric and material properties of the beam are chosen as the same as they were in the previous case. It is clear that the load applied to cracked beam should be less than the first critical buckling load, therefore similar to first case, as a first step a buckling analysis is carried out.

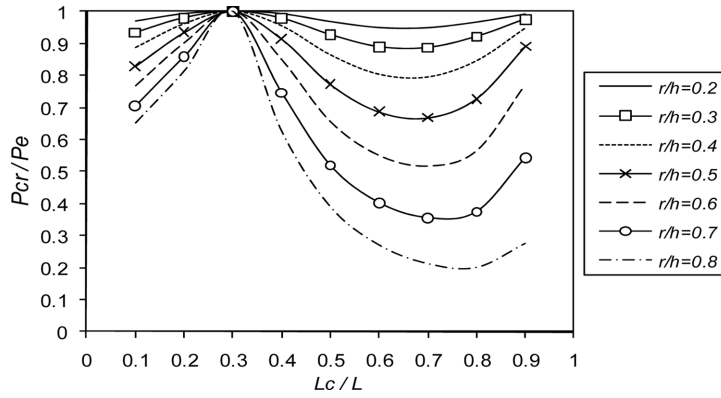


Fig. 12 First non-dimensional buckling loads of cracked beam with respect to different crack locations (L_c/L) and crack ratios (r/h)

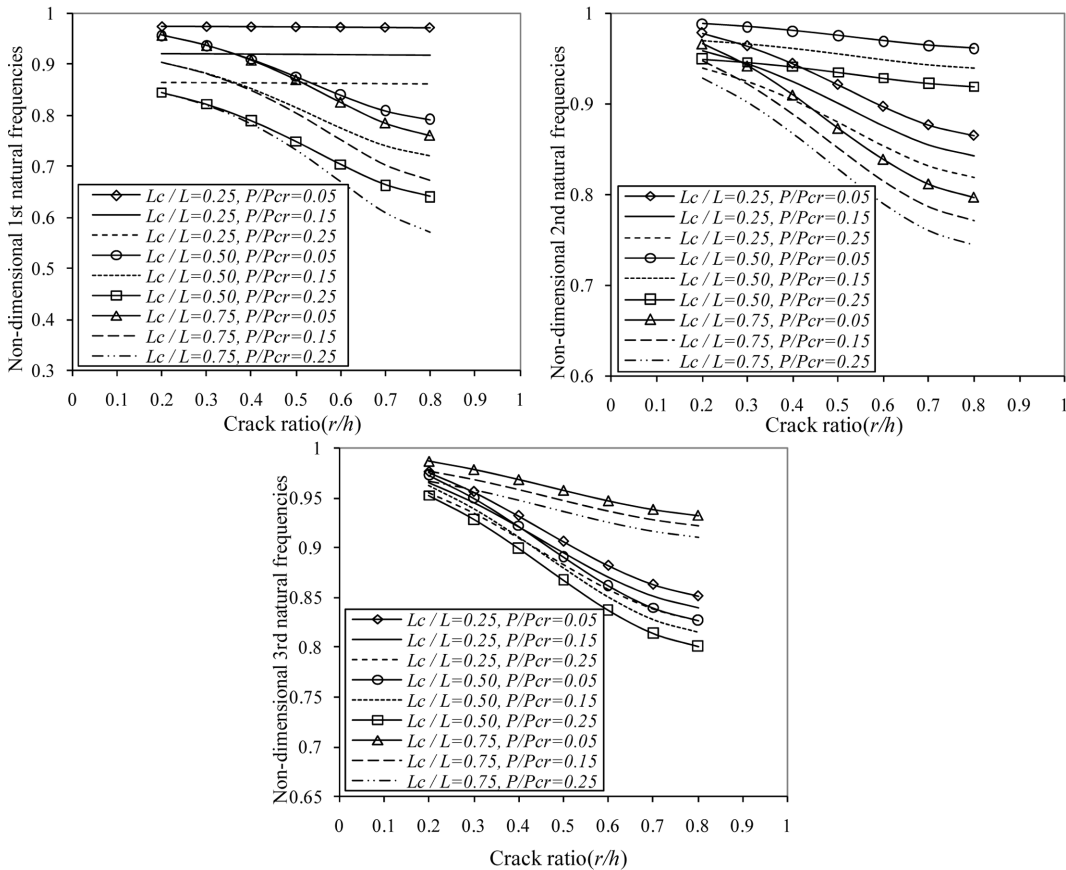


Fig. 13 First, second and third non-dimensional natural frequencies of axially loaded fixed-pinned cracked beam with respect to different applied axial loads (P/P_{cr}), crack locations (L_c/L) and crack ratios (r/h)

3.2.1 Buckling analysis of fixed-pinned cracked beam

The fundamental critical buckling load of the fixed-pinned intact beam can be found by using the Euler Formula as

$$P_e = \frac{\pi^2 EI}{(0.7L)^2} \tag{30}$$

Eq. (28) gives the primary critical buckling load of cracked beam. Fig. 12 illustrates the variation of the first non-dimensional buckling load (P_{cr}/P_e) of cracked and intact beam with respect to different crack location and ratios. A crack positioned near the 70% of the beam length ($L_c/L = 0.7$) causes up to 80% reductions in the buckling load. Quite the opposite, if the crack is located ($L_c/L = 0.3$) near the inflection points (moment zero points of the corresponding intact beams) and is quite big ($r/h = 0.8$) it has almost no effect on the buckling load of the beam.

3.2.2 Vibration of axially loaded fixed-pinned cracked beam

Vibration analysis of a fixed-pinned cracked beam subjected to an axial load P is carried out by using Eq. (25). The variation of the first, second and third non-dimensional natural frequencies of axially loaded fixed-pinned cracked beam with respect to different applied axial load ratios (P/P_{cr}),

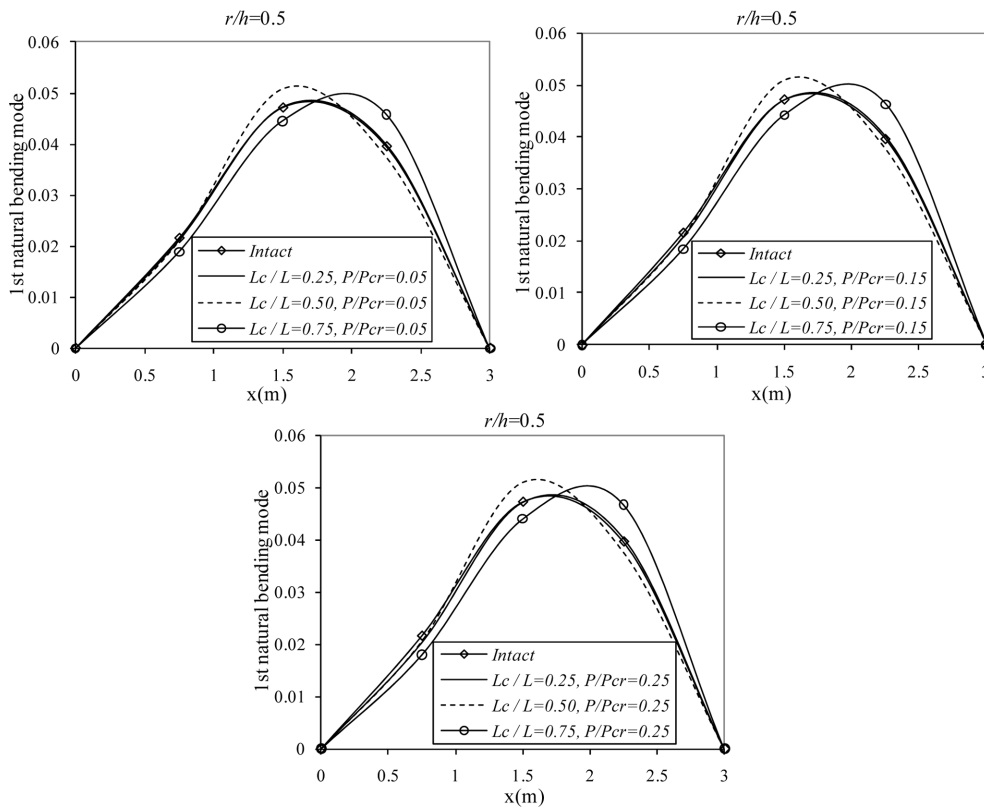


Fig. 14 First mode shapes of the axially loaded fixed-pinned cracked beam with respect to applied axial loads $P/P_{cr} = 0.05, 0.15, 0.25$, crack locations $L_c/L = 0.25, 0.50, 0.75$ and crack ratio $r/h = 0.5$ for the intact and loaded cracked beams

crack locations (L_c/L) and crack ratios (r/h) have been given in the Fig. 13. Applied axial load, crack locations and ratios have effects on the natural frequencies of the beam. While a crack located ($L_c/L = 0.25$) near to inflection point causes less effects on the natural frequencies, a crack located at the middle ($L_c/L = 0.50$) and near the end of the beam ($L_c/L = 0.75$) result in more reductions in the first, third and first, second natural frequencies, respectively. Figure shows that applied axial loads with the ratios of 5%, 15% and 25% ($P/P_{cr} = 0.05, 0.15$ and 0.25) decrease the first natural frequencies of the fixed-pinned beam by 3%, 8% and 14% compared to unloaded beam, respectively for a crack location $L_c/L = 0.25$ and crack ratio $r/h = 0.5$. The same crack results in reductions about 8%, 10%, 12% and 9.5%, 10.5%, 11.5% in the second and third natural frequencies for the applied axial load ratios of 5%, 15% and 25% ($P/P_{cr} = 0.05, 0.15$ and 0.25), respectively.

The effects of cracks at different locations can be explored from the figure. For a beam with a crack ($L_c/L = 0.50, r/h = 0.5$), axial loads with the ratios of 5%, 15% and 25% ($P/P_{cr} = 0.05, 0.15$ and 0.25) decrease the first natural frequencies about 12.5%, 18.5% and 25%. As the same crack ($L_c/L = 0.50, r/h = 0.5$) causes drops about 2.5%, 4.5%, 6.5% and 11%, 12%, 13% in the second and third natural frequencies for the applied axial loads of 5%, 15% and 25% ($P/P_{cr} = 0.05, 0.15$ and 0.25), respectively. For the fixed-pinned beam a crack ($L_c/L = 0.75, r/h = 0.5$) causes

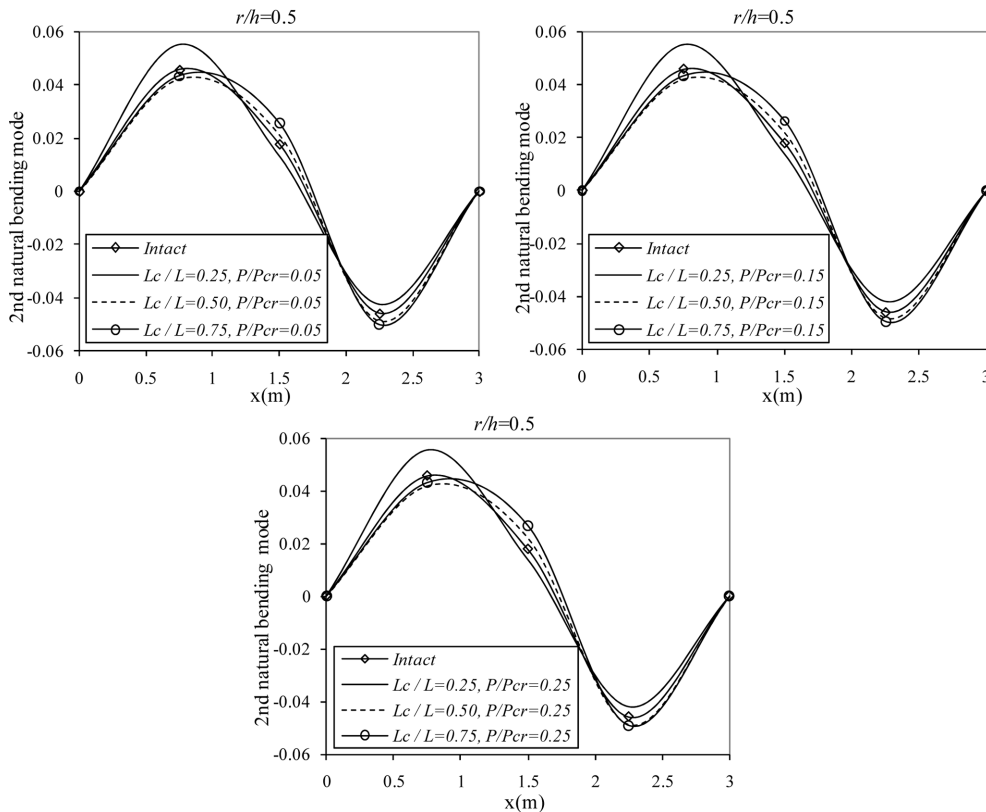


Fig. 15 Second mode shapes of the axially loaded fixed-pinned cracked beam with respect to applied axial loads $P/P_{cr} = 0.05, 0.15, 0.25$, crack locations $L_c/L = 0.25, 0.50, 0.75$ and crack ratio $r/h = 0.5$ for the intact and loaded cracked beams

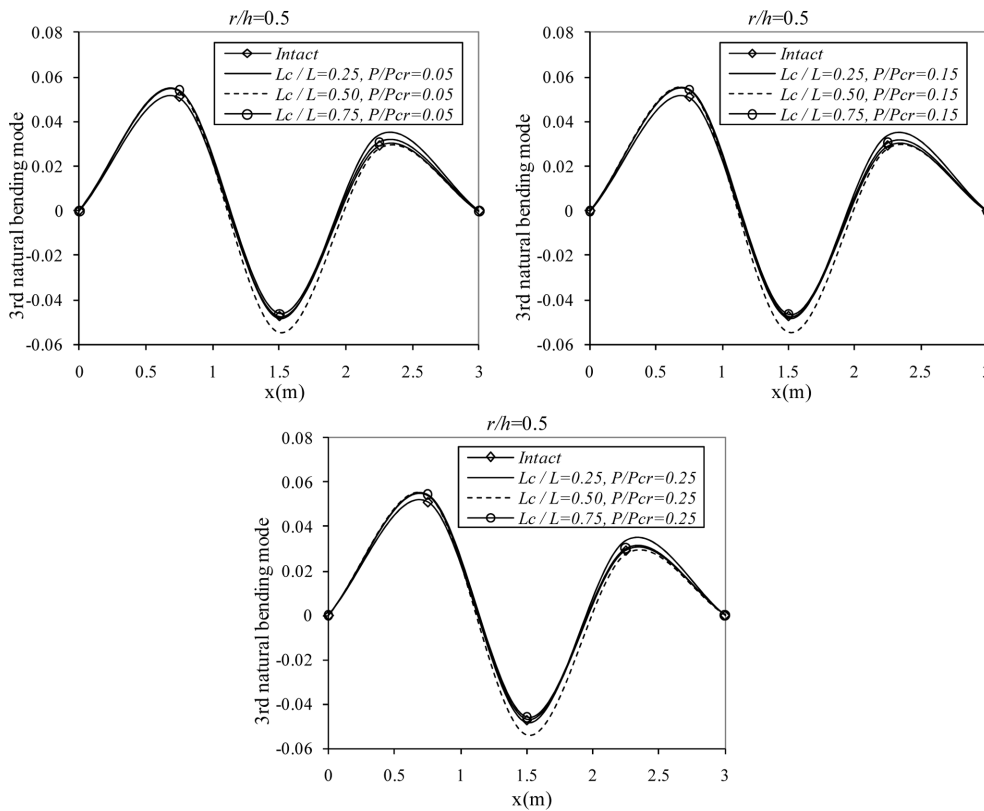


Fig. 16 Third mode shapes of the axially loaded fixed-pinned cracked beam with respect to applied axial loads $P/P_{cr} = 0.05, 0.15, 0.25$, crack locations $L_c/L = 0.25, 0.50, 0.75$ and crack ratio $r/h = 0.5$ for the intact and loaded cracked beams

decreasing about 13%, 20%, 27%; 13%, 15%, 17% and 4.5%, 5.5%, 6.5% in the first, second and third natural frequencies for the applied axial load ratios of 5%, 15% and 25% ($P/P_{cr} = 0.05, 0.15$ and 0.25), respectively.

Deviation of the first, second and third mode shapes of the fixed-pinned beam with respect to crack locations $L_c/L = 0.25, 0.50, 0.75$, applied axial load ratios $P/P_{cr} = 0.05, 0.15, 0.25$ and crack ratio $r/h = 0.5$ for the intact and loaded cracked beams are illustrated in Figs. 14-16. From these figures it can be clearly seen that applied axial load ratios, crack locations and ratios play important role on the variation of mode shapes.

4. Conclusions

In this paper component mode synthesis technique accompanied by the finite element method is applied for the first time to the vibration analysis of cracked beams subjected to compressive axial loading. Using the presented technique a non-linear problem separated into two linear subsystems. As the whole structure is detached from the crack section, making use of the present approach is alleged to propose a proficient technique capable of exploring the non-linear interface effects such

as contact and impact that occur if crack closes. Prior to vibration of axially loaded cracked beam, a buckling analysis is completed to find the critical buckling loads. Throughout the study only elastic buckling is considered. It is shown that crack ratios and locations affect the buckling behaviour of the beam. As expected, larger cracks have produced higher drops in the buckling load.

It is presented that applied compressive axial load ratios, crack locations and ratios play important role on the variation of natural frequencies and mode shapes. Cracks and applied load decrease the overall stiffness of the beam and as a consequence the dynamical characteristics of the beam are modified. Higher applied axial load ratios have produced more reductions in the natural frequencies and more changes in the mode shapes.

It is revealed that the knowledge of modal data of cracked beams forms an important aspect in assessing the structural failure. To demonstrate the efficiency of the procedure, outcomes of the presented numerical cases have been compared with earlier studies available in the literature leading to confidence in the validity of this approach. The application of the current work is limited to the vibration analysis of beams with non-propagating open cracks. Some possible extensions of the current study are the analysis of the beams with other cross sections, propagating of cracks, beams with multiple cracks and inclusion of contact and impact effects if the crack closes.

References

- Arbodela-Monsalve, L.G., Zapata-Medina, D.G. and Aristizabal-Ochoa, J.D. (2007), "Stability and natural frequencies of a weakened Timoshenko beam-column with generalized end conditions under constant axial load", *J. Sound Vib.*, **307**, 89-112.
- Aristizabal-Ochoa, J.D. (2007), "Static and dynamic stability of uniform shear beam-columns under generalized boundary conditions", *J. Sound Vib.*, **307**, 69-88.
- Aydin, K. (2007), "Vibratory characteristics of axially loaded Timoshenko beams with arbitrary number of cracks", *J. Vib. Acoust.*, **129**, 341-354.
- Aydin, K. (2008), "Vibratory characteristics of Euler-Bernoulli beams with an arbitrary number of cracks subjected to axial load", *J. Vib. Cont.*, **14**, 485-510.
- Binici, B. (2005), "Vibration of beams with multiple open cracks subjected to axial force", *J. Sound Vib.*, **287**, 277-295.
- Brandon, J.A. and Abraham, O.N.L. (1995) "Counter-intuitive quasi-periodic motion in the autonomous vibration of cracked Timoshenko beams", *J. Sound Vib.*, **185**, 415-430.
- Chasalevris, A.C. and Papadopoulos, C.A. (2008), "Coupled horizontal and vertical bending vibrations of a stationary shaft with two cracks", *J. Sound Vib.*, **309**, 507-528.
- Cheng, Y., Yu, Z., Wu, X. and Yuan, Y. (2011), "Vibration analysis of a cracked rotating tapered beam using the p-version finite element method", *Finite Elem. Anal. Des.*, **47**, 825-834.
- Darpe, A.K. (2007), "Coupled vibrations of a rotor with slant crack", *J. Sound Vib.*, **305**, 172-193.
- Dilena, M. and Morassi, A. (2002), "Identification of crack location in vibrating beams from changes in node positions", *J. Sound Vib.*, **255**, 915-930.
- Dimarogonas, A.D. and Paipetis, S.A. (1983), *Analytical Methods in Rotor Dynamics*, Applied Science Publishers.
- Gounaris, G. and Dimarogonas, A.D. (1988), "A finite element of a cracked prismatic beam for structural analysis", *Comput. Struct.*, **28**, 309-313.
- Gudmundson, P. (1983), "The dynamic behaviour of slender structures with cross-sectional cracks", *J. Mech. Phys. Solids*, **31**, 329-345.
- Hsu, M.H. (2005), "Vibration analysis of edge-cracked beam on elastic foundation with axial loading using the differential quadrature method", *Comput. Meth. Appl. Mech. Eng.*, **194**, 1-17.
- Hurty, W.C. (1965), "Dynamic analysis of structures using substructure modes", *AIAA J.*, **3**, 678-685.

- Irwin, G. (1960), *Fracture Mechanics*, Structural Mechanics, Pergamon Press.
- Kisa, M. (2004), "Free vibration analysis of a cantilever composite beam with multiple cracks", *Compos. Sci. Technol.*, **64**, 1391-1402.
- Kisa, M. and Brandon, J.A. (2000), "Free vibration analysis of multiple open-edge cracked beams by component mode synthesis", *Struct. Eng. Mech.*, **10**, 81-92.
- Kisa, M. and Gurel, M.A. (2007), "Free vibration analysis of uniform and stepped cracked beams with circular cross sections", *Int. J. Eng. Sci.*, **45**, 364-380.
- Kisa, M., Brandon, J.A. and Topcu, M. (1998), "Free vibration analysis of cracked beams by a combination of finite elements and component mode synthesis methods", *Comput. Struct.*, **67**, 215-223.
- Krawczuk, M. (2002), "Application of spectral beam finite element with a crack and iterative search technique for damage detection", *Finite Elem. Anal. Des.*, **38**, 537-548.
- Krawczuk, M. and Ostachowicz, W.M. (1993), "Transverse natural vibrations of a cracked beam loaded with a constant axial force", *J. Vib. Acoust.*, **115**, 524-528.
- Kukla, S. (2009), "Free vibrations and stability of stepped columns with cracks", *J. Sound Vib.*, **319**, 1301-1311.
- Loya, J.A., Rubio, L. and Fernández-Sáez, J. (2006), "Natural frequencies for bending vibrations of Timoshenko cracked beams", *J. Sound Vib.*, **290**, 640-653.
- Mei, C., Karpenko, Y., Moody, S. and Allen, D. (2006) "Analytical approach to free and forced vibrations of axially loaded cracked Timoshenko beams", *J. Sound Vib.*, **291**, 1041-1060.
- Morassi, A. (2001), "Identification of a crack in a rod based on changes in a pair of natural frequencies", *J. Sound Vib.*, **242**, 577-596.
- Pandey, U.K. and Benipal, G.S. (2011), "Bilinear elastodynamical models of cracked concrete beams", *Struct. Eng. Mech.*, **39**, 465-498.
- Patel, T.H. and Darpe, A.K. (2009), "Coupled bending-torsional vibration analysis of rotor with rub and crack", *J. Sound Vib.*, **326**, 740-752.
- Patil, D.P. and Maiti, S.K. (2003), "Detection of multiple cracks using frequency measurements", *Eng. Fract. Mech.*, **70**, 553-572.
- Qian, G.L., Gu, S.N. and Jiang, J.S. (1990), "The dynamic behaviour and crack detection of a beam with a crack", *J. Sound Vib.*, **138**, 233-243.
- Rizos, P.F., Aspragathos, N. and Dimarogonas, A.D. (1990), "Identification of crack location and magnitude in a cantilever beam from the vibration modes", *J. Sound Vib.*, **138**, 381-388.
- Ruotolo, R., Surace, C., Crespo, P. and Storer, D. (1996), "Harmonic analysis of the vibrations of a cantilevered beam with a closing crack", *Comput. Struct.*, **61**, 1057-1074.
- Shifrin, E.I. and Ruotolo, R. (1999), "Natural frequencies of a beam with an arbitrary number of cracks", *J. Sound Vib.*, **223**, 409-423.
- Takahashi, I. (1998), "Vibration and stability of a cracked shaft simultaneously subjected to a follower force with an axial force", *Int. J. Solids Struct.*, **35**, 3071-3080.
- Viola, E., Federici, L. and Nobile, L. (2001), "Detection of crack location using cracked beam element method for structural analysis", *Theor. Appl. Fract. Mec.*, **36**, 23-35.
- Viola, E., Ricci, P. and Aliabadi, M.H. (2007), "Free vibration analysis of axially loaded cracked Timoshenko beam structures using the dynamic stiffness method", *J. Sound Vib.*, **304**, 124-153.
- Wang, Q. (2004), "A comprehensive stability analysis of a cracked beam subjected to follower compression", *Int. J. Solids Struct.*, **41**, 4875-4888.
- Yang, J., Chen, Y., Xiang, Y. and Jia, X.L. (2008), "Free and forced vibration of cracked inhomogeneous beams under an axial force and a moving load", *J. Sound Vib.*, **312**, 166-181.
- Yuen, M.M.F. (1985), "A numerical study of the eigenparameters of a damaged cantilever", *J. Sound Vib.*, **103**, 301-310.
- Zheng, D.Y. and Fan, S.C. (2003), "Vibration and stability of cracked hollow-sectional beams", *J. Sound Vib.*, **267**, 933-954.
- Zheng, D.Y. and Kessissoglou, N.J. (2004), "Free vibration analysis of a cracked beam by finite element method", *J. Sound Vib.*, **273**, 457-475.